Numerical Modelling of Aircraft Evacuations

Abdulrahman Alabdulkareem
Electrical Engineering and Computer Science
arkareem@mit.edu

Joseph Chiapperi
Aeronautics and Astronautics
chiapper@mit.edu

Spencer Taylor
Aeronautics and Astronautics
svtaylor@mit.edu

***Abstract*—The FAA regulation for safe aircraft evacuations requires a demonstration under specific conditions. This paper demonstrates how a numerical model can be used to simulate a much wider range of conditions. This numerical model is created as an equivalent circuit with non-linear constitutive equations. Employing the model on an example baseline configuration shows the location of bottlenecks and shows the relative impact of obstacles in the evacuation path. When paired together, a physical demonstration and numerical model can more effectively ensure that an aircraft is capable of a safe evacuation in all conditions, compared to a physical demonstration alone.**

I. Introduction & Motivations

The FAA requires that passenger aircraft are able to be evacuated in 90 seconds [1]. The time requirement is the same no matter the aircraft size, including the smallest regional turboprops and the largest airliner, the Airbus A380 (Fig. 1). This rule was implemented in 1967 following the investigation of a 1965 accident in Salt Lake City [2]. Although periodically updated, the Department of Transportation, Office of Inspector General has found that the regulation lacks a connection to gathered data and is considerably out-of-date [2].

This project attempts to make a simplified model of the aircraft evacuation process. The FAA regulations state that an aircraft manufacturer must demonstrate effective evacuation under one set of conditions. We can use our model to assess an aircraft under a much wider variety of conditions, reducing the risk of gaps in the regulations.

A prior model addressing this application was made by Poudel, et. al. [3] This model uses Cellular Automata (CA) to represent each passenger. The governing equations are the defined by the interactions between passengers during an evacuation. Such a system allows for a high degree of flexibility, since each passenger can be defined by their own characteristics, corresponding to age, health, mobility, etc. In this paper, we choose to place a greater focus on the parameters of the aircraft, such as the position of emergency exits and the presence of obstructions.

Other crowd simulation techniques include those used by Wang and Luh [4], Adrian et. al. [5] and Kabalan et. al. [6]. These all seek to model the phenomenon of "bottlenecks" in crowd motion. Of these, Wang and Luh [4] is simplest to understand as it is a fluid-based model with compressible flow equations. These models do a good job of characterizing the movement of crowds in large two dimensional spaces. An aircraft however, is a much more restricted space, essentially limiting the crowd movement to a single-file queue. We therefore implement equations which are similar to compressible flow, but take advantage of this simplified space.

Fig. 1: The 90-second Evacuation Requirement is the same for all passenger aircraft, including the Airbus A380, the largest passenger jet in operation. Image: [3]

II. Problem formulation

The aircraft is divided into a series of "compartments"; including each grouping of seats and each intersection between seat rows and the aisle(s). Each of these compartments is a node in the state space model. The state variable for each node, denoted by x_i, is a value for how tightly packed the compartment is. Therefore, an aircraft with people evenly distributed throughout might have a state space vector of one in every dimension (or scaled by some scalar), even if the compartments are different sizes.

The ordering of these nodes is a modified row-wise order. For a given row, Node 1 is the left set of seats, Node 2 is the right set of seats, Node 3 is the aisle, Node 4 is the left set of seats in the next row, and so on. This ordering results in a matrix with a maximum band of 3 and no potential for fill-ins. In a twin-aisle aircraft, the ordering for each row should be left seat, right seat, center seat, left aisle, right aisle. This has a maximum band of 5, and about 8 fill-ins per row. In both cases, a simple left-to-right ordering will only change the fill-in pattern, and not the band. In every case, no matter the size, ordering length-wise first is worse because the band changes with aircraft size.

The nodes are connected by resistors representing the interface between compartments. The resistance is equal to the amount of time it takes a person to pass through that interface, without being "rushed." Thus, the resistors connecting the seats to the aisle will have a higher resistance than the resistors along the aisle itself, and so on. Although these segments are referred to as "resistors", they exhibit non-linear behavior. The segments have a maximum flow rate, which is the maximum number of people that can move through the interface per second. The details of the implementation of this non-linearity, along with a simple path-finding setup are discussed with the constitutive equations.

Finally, each node has a capacitance which specifies the size of the compartment. The value is the number of people that would fit comfortably in the space. For seat rows, this is simply the number of seats, and for aisles this value is 2. Figure 2 in Section V shows an example single-aisle configuration with 30 rows and 2 exits, roughly equivalent to a Boeing 737 with single-class seating.

The conservation equation states that the rate of change of the number of people at a node is equal to the difference between the number of people leaving the node and the number of people entering the node. This conservation law is represented by Eqn. 1.

$$C_i \frac{dx_i}{dt} = \Sigma I_{ij} \tag{1}$$

Here, C_i is the capacitance of Node i, x_i is the state variable for Node i, t is time, and I_{ij} is the current into Node i from Node j, which is summed for all Nodes, j connecting to Node i.

The constitutive equation specifies how much current flows between any two given nodes. This relationship is roughly linear for low flow rates, but tapers off at some maximum. This idea of a maximum possible flow rate stems from compressible flow equations, as is suggested by Wang and Luh [4]. We approximate this relationship as a shifted and scaled Sigmoid equation. The specific function is shown in Eqn. 2. Here, I_{ij} is the flow of people from Node i to Node j, x_i is the state variable at Node i, x_j is the state variable at Node j, a_{ij} is the maximum flow rate for the segment between Nodes i and j, and R_{ij} is the resistance of the segment between Nodes i and j.

$$I_{ij} = \frac{2a_{ij}}{1 + e^{\frac{2(x_j - x_i)}{a_{ij} R_{ij}}}} - a_{ij} \tag{2}$$

This Sigmoid function is shaped such that flow rate is roughly linear with respect to the difference in state variable at low flow rates, with the slope defined as $1/Resistance$, and tapers off to the maximum rate, a. This shape is consistent with what we would expect from crowd and queue movement, and stems from the comparison to compressible flow. It is also continuous and continuously differentiable. The values of R, a, C, and the topographical information are all contained in the parameter vector, p.

We implement a simple path-finding system by making the resistors non-bi-directional. The Sigmoid function in Eqn. 2 is clipped to zero, such that flow is not allowed in the direction away from the nearest exit. In reality, this corresponds to passengers initially choosing an exit, and then sticking to that choice until they evacuate. The resulting function is no longer continuously differentiable, so care must be taken in the Newton solvers later on.

The input vector, u, is technically empty. In the code however, we use the input vector as a means to specify the initial state vector.

The output of the system, y, is the total number of people on the aircraft, calculated with Eqn. 3, where C^T is the vector of the capacitances of each node, and x is the state vector.

$$y = C^T x \tag{3}$$

We assess the effectiveness of the evacuation, and the impact of any parameter changes, by noting the time at which this output, y, drops below a threshold, ϵ, which we set to 0.1.

III. Fundamental Numerical Methods

Algorithm 1 evalf

```
function evalf_linear(x, u, p)
    return p.nodalMatrix * x + u
function evalf_sigmoid(x, u, p)
    r, a ← p.resistors, p.upperlimits
    constit_eq ← sigmoid_upper(p.E' * x, r, a)
    if p.shortestPathMode then
        opp ← sign(p.shortpath). * sign(constit_eq)
        constit_eq(opp == −1) = 0
    dx/dt ← (−p.E * constit_eq)./p.C
    return dx/dt
function analytical_jacobian(x, u, p)
    r, a ← p.resistors, p.upperlimits
    sig ← sigmoid(2 * (p.E' * x)./(a. * r))
    constit_eq ← (4/r). * sig. * (1 − sig)
    constit_eq ← diag(constit_eq) * p.E'
    if p.shortestPathMode then
        activ ← 2 * a. * sig − a
        opp ← sign(p.shortpath). * sign(activ) == −1
        constit_eq(opp, :) = 0
    Jacobian ← diag(1./p.C) * (−p.E * constit_eq)
    return Jacobian
function sigmoid_upper(dx, r, a)
    return 2 * a. * sigmoid(2 * dx./(a. * r)) − a
function sigmoid(x)
    return 1/(1 + exp(−x))
```

Algorithm 2 Newton_solve

```
Ensure: x^k is the solution of f(x^k, p, u) = 0 or diverges
function NEWTON_SOLVE(f(·), j(·), x^0, p, u)
    k ← 0
    f^0 ← f(x^0, p, u)
    repeat
        Jf ← j(x^k, p, u)
        dx ← −1. * Jf \ f^k
        x^{k+1} ← x^k + dx
        k ← k + 1
        f^k ← f(x^k, p, u)
        if min(‖f^k‖∞, ‖dx‖∞, ‖dx‖∞ / max(abs(x^k))) < 10^−8 then
            return x^k, k
    until k > 10
    return diverged
```

For our core function $evalf$ we use a Nodal-Branch form to calculate the gradients across each of the nodes at any given state. The matrix E is the Node-to-Branch matrix containing a row for each resistor with a $+1$ value for an outgoing connection and a -1 for an incoming connection.

If the simulation is run using path-finding mode, the $evalf$ function only changes slightly to clip flow through resistors that is opposite to the shortest path. This is achieved through a pre-computed vector $p.shortpath$ that contains either a $+1$ or a -1 for each resistor depending on which direction through this resistor leads to the nearest exit. Assigning a 0 value to this vector allows flow through either direction of the resistor. Additionally, through clever assignment of 0's in the $shortpath$ vector, we can achieve a simulated lack of knowledge of where the nearest exit is which leads to random path taking until an exit is within viewing distance. Additionally, due to the elegant mathematical properties of the sigmoid and the vectorized implementation of the path-finding, we were able to implement a vectorized implementation of the analytical jacobian to our system that is very efficient.

IV. The Technical Challenge

For our technical challenge, we chose to implement a trapezoidal ODE integrator with dynamic time stepping to reduce the solve time of our system. The pseudocode as given previously in the 16.910/6.7300 course [7], adapted for our system, is shown in Alg. 3.

Algorithm 3 Trapezoidal Integrator with Dynamic Time Stepping

Require: $x(t^0) = x^0$
Ensure: x is the solution of $\frac{dx}{dt} = f(x, p, u)$
  function $\textsc{Trap}(f(\cdot), j(\cdot), x^0, p, u, \Delta t, maxt, stop(\cdot))$
    $l \leftarrow 1, t^0 \leftarrow 0$
    repeat
      $\gamma \leftarrow x^{l-1} + \frac{\Delta t}{2} f$
      $N.F \leftarrow @(x)\ x - \frac{\Delta t}{2} f(x, u, p) - \gamma$
      $N.J \leftarrow @(x)\ I - \frac{\Delta t}{2} j(x, u, p)$
      $N.x^0 \leftarrow x^l + \Delta t f(\cdot)$
      $x^l \leftarrow \textsc{Newton\_Solve}(N.F, N.J, N.x^0, p, u)$
      if Newton converged in fewer than 5 iterations **then**
        $l \leftarrow l + 1, t^l \leftarrow t^{l-1} + \Delta t$
        $\Delta t \leftarrow 1.8 \Delta t$
      else if Newton converged **then**
        $l \leftarrow l + 1, t^l \leftarrow t^{l-1} + \Delta t$
        $\Delta t \leftarrow 1.1 \Delta t$
      else if Newton did not converge **then**
        $\Delta t \leftarrow \frac{\Delta t}{2}$
      if $\Delta t > maxt$ **then**
        $\Delta t \leftarrow maxt$
    until $stop(\cdot)$
    return $[x^0\ x^1\ x^2\ ...\ x^n], [t^0\ t^1\ t^2\ ...\ t^n]$

When implementing the trapezoidal ODE integrator with dynamic time stepping for our standard configuration (c.f. Fig. 2), we see that initially, as passengers are quickly evacuating the plane, the ODE integrator requires small timestep Δt given the fast change in the total number of passengers per unit time. As time increases and passengers have filled nearby empty nodes, the trapezoidal integrator is able to use larger Δt given the lower relative rate of change in the number of passengers on board. This dynamic change in Δt results in a faster solve time than the typical Forward Euler integrator when comparing both and allowing for an error of $< \pm 0.1$ seconds.

V. Results

First, we assess a baseline configuration and several smaller configurations to show that the model is working as expected. Figure 2 shows the density of people on the aircraft partway through an evacuation. Here we note that people are generally clustered away from the exits.

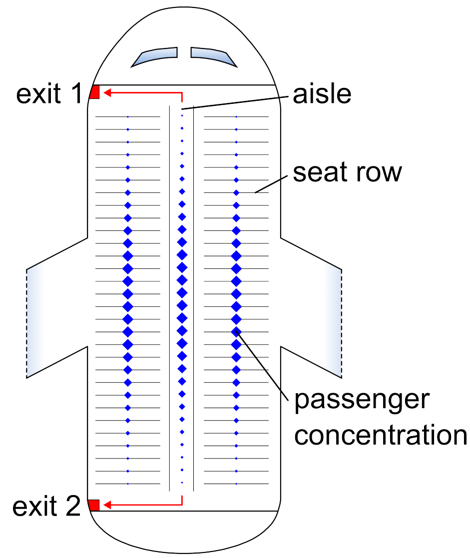

Fig. 2: The relative density of people on board the aircraft midway through an evacuation. For a 30 row example with two exits. Note the relative density of people away from the exits.

We assess the impact of the resistances of each segment in the network. The importance here is that the FAA regulations governing safe evacuations specify that the demonstration must be carried out with 50% of the onboard baggage distributed throughout the cabin as obstructions. However, we expect there to be a larger impact on evacuation time from some locations than from others. Identifying these "choke points" and the relative difference between an even resistance distribution and a concentrated distribution can show if further detail is needed in the regulations or not.
The parameters for the "baseline" configuration (shown in Fig. 2) are defined in Tables I and II.

TABLE I: Baseline Configuration Resistances

Segment	Resistance (sec.)	Max. Flow(people per sec.)
seat-to-aisle	0.4	1
aisle-to-aisle	0.1	1
front & rear exits	0.05	1
emergency exits	0.05	1

TABLE II: Baseline Configuration Capacitances

Node	Capacitance (No. of people)
seat row	3
aisle junction	2
emergency exit rows	3

The evolution of the number of people aboard the aircraft overtime is shown for four configurations in Fig. 3; the baseline with no obstacles, an obstacle at the front exit, and an obstacle in the middle of the aircraft, and an obstacle in a seat row.

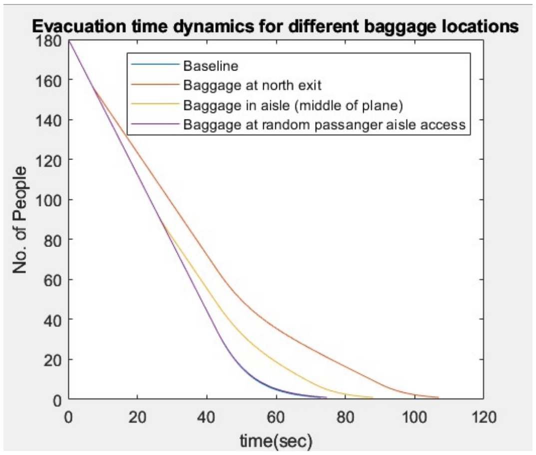

Fig. 3: Time Evolution of No. of People Aboard the Aircraft for Four Configurations

The efficiency of the model is demonstrated by increasing the size of the network to an arbitrarily large size, with 100 rows, and comparing the memory usage and execution time. The largest size we could ever expect for this model is 84 rows, which corresponds to an Airbus A380 with a one-class configuration. We find that the system still runs quickly, especially if the dynamic trapezoidal method is employed. We can increase the speed even more if we relax the accuracy requirement, which may be suitable for a comparative analysis, but not for an absolute analysis.

VI. Technical Discussion

Figure 2 shows that midway through an evacuation, the model predicts that people will be clustered away from the exits. This is consistent with real-world experiences during a normal deplaning procedure at an airport. The front rows near the exit empty first, and people are clustered at the back until the rows in front of them clear.

Smaller cases were also run to verify the pathfinding setup used in the model. When one person is placed in an empty plane, they immediately proceed to the nearest exit. When people are equidistant to two exits, they diverge to both.

Figure 3 shows the time evolution of the number of people aboard the aircraft throughout the evacuation. We observe that the trend is nearly linear for most of the time before smoothly reaching zero as the last few people trickle out. This is consistent with other models which simulate building evacuations [8]. The maximum flow of the aisle is reached, and the evacuation progresses linearly until the flow falls below this limit.

Figure 3 also shows that the presence of obstacles does indeed slow down the evacuation, and that this impact is highly dependent on the location of the obstacle. Obstacles in the aisle slow people down more than in the seats, and the worst location is in front of the exit.

Finally, we note that there are some behaviors which are inconsistent with what would be expected in reality. This includes the non-linear evacuation rate near the end of the time evolution. This is expected with our model, since it is based on diffusion at low flow rates. However, we do not expect this behavior to occur in a real evacuation. People would exit as quickly as possible, regardless of the density of people behind them. Additionally, our constitutive model does not allow for people to change their minds if another, farther exit clears up. This indicates that there is a need for further model refinement before a tool such as this could be useful.

VII. Ethics & Limitations

The stakeholders for this system include airlines/operators, airframers (i.e. Boeing, Airbus), regulators (i.e. FAA, EASA), and passengers. The primary risk for airlines, passengers and regulators is for an aircraft to be falsely marked as “safe”. If this is the case, passengers risk being injured or killed, and airlines and operators risk being held responsible for the accident. The primary risk for airframers is for an aircraft to be falsely marked as “unsafe”, leading to unnecessary development in order to meet this excessive requirement. The most recent FAA strategic plan [9] states that safety and operational excellence are two of their primary missions. They also discuss how the evolving aviation landscape requires data-driven analysis to replace legacy conventions.

With these risks in mind, we make it clear that this model, or any similarly developed model of a higher fidelity, should not be used as a sole means to demonstrate the safety of an aircraft during evacuation. It should instead be used in conjunction with the physical demonstrations currently required, in keeping with both the FAA strategic plan [9] and the process by which the FAA changes regulations [10]. This procedure ensures that all stakeholders are aware of the proposed change and may provide input so that the regulation can best serve all parties. The final result may create slightly different regulations for each different aircraft, but there is precedent for this action. The Boeing 747 for example, requires special rules to be made concerning the evacuation of its upper deck area [11].

Finally, it is important to identify the limitations of the model discussed in this paper. The primary limitation is that it treats all passengers the same, since the only parameters are to do with the aircraft layout. This is not true in practice, as aircraft must be proven safe not only for healthy, able passengers, but also for those who are elderly or disabled. Additionally, we have only calibrated the model to be accurate in its sole output of the total number of people aboard the aircraft. The nature of the chosen constitutive equations means that the distribution of people at any given time may not reflect reality. For example it allows for a non-integer number of people to occupy a node. We therefore restrict the displayed outputs accordingly.

VIII. Conclusions

We use a modified circuit model to simulate an aircraft evacuation. We use non-linear resistors based on a Sigmoid function and a simple path finding system to drive people to their nearest exit. This model correctly shows how people are clustered away from an exit while they wait for rows in front of them to exit. It also roughly corresponds to available data for building evacuations. The model is used to evaluate the impact of obstacles at different locations in the aircraft and it is found that obstacles have a larger impact on evacuation time the closer they are to an exit. Finally, we note that there are some behaviors which do not match reality, such as a diffusion action at low flow rates, which indicates the need for further model refinement before such a tool could be useful.

References

[1] Emergency Evacuation, 14 CFR Appendix J to Part 25. 2011. Available: https://www.govinfo.gov/app/details/CFR-2011-title14-vol1/CFR-2011-title14-vol1-part25-appJ

[2] Department of Transportation, Office of Inspector General, "FAA's Process for Updating Its Aircraft Evacuation Standards Lacks Data Collection and Analysis on Current Evacuation Risks," Washington, DC, USA, 2020 [Online]. Available: https://www.oig.dot.gov/sites/default/files/FAA%20Oversight%20of%20Aircraft%20Evacuations%20Final%20Report%20-%2009-16-20.pdf

[3] M. Poudel, B. Chaudhury, K. Sharma, P. Tabakov, and F. Mora-Camino, "GPU based Computational Simulation of Aircraft Evacuation: Temporal and Spatial Analysis," Transportation Research Procedia, vol. 29, pp. 356–365, Jan. 2018, doi: 10.1016/j.trpro.2018.02.032.

[4] P. Wang and P. B. Luh, "Fluid-Based Analysis of Pedestrian Crowd at Bottlenecks," arXiv:1309.2785 [phyics.soc-ph], Sept. 2013.

[5] J. Adrian, A. Seyfried, and A. Sieben, "Crowds in front of bottlenecks at entrances from the perspective of physics and social psychology," Journal of The Royal Society Interface, vol. 17, no. 165, p. 20190871, Apr. 2020, doi: 10.1098/rsif.2019.0871.

[6] B. Kabalan, P. Argoul, A. Jebrane, G. Cumunel, and S. Erlicher, "A crowd movement model for pedestrian flow through bottlenecks," Ann. Solid Struct. Mech., vol. 8, no. 1, pp. 1–15, Dec. 2016, doi: 10.1007/s12356-016-0044-3.

[7] Luca Daniel, "2.091/6.336/16.910 Introduction to Numerical Simulation" MIT, Graduate Course, Fall 2018.

[8] M. Xiao et al., "Simulation of emergency evacuation from construction site of prefabricated buildings," Sci Rep, vol. 12, no. 1, Art. no. 1, Feb. 2022, doi: 10.1038/s41598-022-06211-w.

[9] Flight Plan 21; The FAA Strategic Plan for the 21st Century, Washington, DC, USA, 2022 [Online]. Available: https://www.faa.gov/general/flight-plan-21/fp21

[10] General Rulemaking Procedures, 14 CFR Part 11. 2020. Available: https://www.ecfr.gov/current/title-14/chapter-I/subchapter-B/part-11/subpart-A

[11] Special Conditions: Boeing Model 747-8 Airplanes; Stairway Between the Main Deck and Upper Deck, 76 FR 31451. 2011. Available: https://www.federalregister.gov/documents/2011/06/01/2011-13433/special-conditions-boeing-model-747-8-airplanes-stairway-between-the-main-deck-and-upper-deck